



Design and synthesis of novel pyrimido[4,5-*b*]azepine derivatives as HER2/EGFR dual inhibitors



Youichi Kawakita*, Masaki Seto, Tomohiro Ohashi, Toshiya Tamura, Tadashi Yusa, Hiroshi Miki, Hidehisa Iwata, Hidenori Kamiguchi, Toshimasa Tanaka, Satoshi Sogabe, Yoshikazu Ohta, Tomoyasu Ishikawa*

Pharmaceutical Research Division, Takeda Pharmaceutical Co., Ltd, 26-1, Muraoka-Higashi 2-chome, Fujisawa, Kanagawa 251-8555, Japan

ARTICLE INFO

Article history:

Received 23 December 2012

Revised 8 February 2013

Accepted 11 February 2013

Available online 22 February 2013

Keywords:

HER2

EGFR

Pyrimido[4,5-*b*]azepine

ABSTRACT

A novel 7,6 fused bicyclic scaffold, pyrimido[4,5-*b*]azepine was designed to fit into the ATP binding site of the HER2/EGFR proteins. The synthesis of this scaffold was accomplished by an intramolecular Claisen-type condensation. As the results of optimization lead us to 4-anilino and 6-functional groups, we discovered 6-substituted amide derivative **19b**, which has a 1-benzothiophen-4-yloxy group attached to the 4-anilino group. An X-ray co-crystal structure of **19b** with EGFR demonstrated that the N-1 and N-3 nitrogens of the pyrimido[4,5-*b*]azepine scaffold make hydrogen-bonding interactions with the main chain NH of Met793 and the side chain of Thr854 via a water-mediated hydrogen bond network, respectively. In addition, the NH proton at the 9-position makes an additional hydrogen bond with the carbonyl group of Met793, as we expected. Compound **19b** revealed potent HER2/EGFR kinase (IC₅₀: 24/36 nM) and BT474 cell growth (GI₅₀: 18 nM) inhibitory activities based on its pseudo-irreversible (PI) profile.

© 2013 Elsevier Ltd. All rights reserved.

1. Introduction

The targeting of human epidermal growth factor receptor 2 (HER2 or ErbB-2/neu) and epidermal growth factor receptor (EGFR or HER1/ErbB-1) by tyrosine kinase inhibitors (TKIs) is an attractive approach for cancer therapy.¹ Several ATP-competitive HER2/EGFR TKIs are currently in clinical trials or have been approved for commercial use.² We previously reported a series of pyrrolo[3,2-*d*]pyrimidine derivatives as potent HER2/EGFR dual kinase inhibitors leading to the clinical candidate TAK-285 (Fig. 1).³ In addition, we have determined X-ray co-crystal structures of TAK-285 with both HER2 and EGFR.^{3,4}

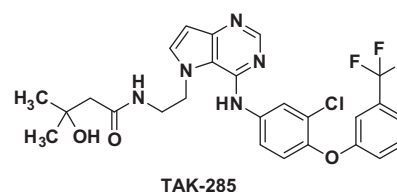


Figure 1. Chemical structure of TAK-285.

Abbreviations: ¹H NMR, proton nuclear magnetic resonance; DMF, *N,N*-dimethylformamide; EGFR, epidermal growth factor receptor; EDC, 1-ethyl-3-(3-dimethylaminopropyl)carbodiimide hydrochloride; EtOAc, ethyl acetate; EtOH, ethanol; GI, growth inhibitory; HCl, hydrochloric acid; HER2, human epidermal growth factor receptor 2; HOBt, 1-hydroxybenzotriazole monohydrate; HPLC, high-performance liquid chromatography; IC, inhibitory concentration; K₂CO₃, potassium carbonate; MgSO₄, magnesium sulfate; MS, mass spectroscopy; NaOH, sodium hydroxide; PI, pseudo-irreversibility; ppm, parts per million; Pd/C, palladium on carbon; SAR, structure-activity relationships; THF, tetrahydrofuran; TKIs, tyrosine kinase inhibitors.

* Corresponding authors. Tel.: +81 466 32 1249; fax: +81 466 29 4450 (Y.K.); tel.: +81 466 32 1155; fax: +81 466 29 4449 (T.I.).

E-mail addresses: youichi.kawakita@takeda.com (Y. Kawakita), tomoyasu.ishikawa@takeda.com (T. Ishikawa).

All of the reported small molecule inhibitors share the common hinge binder characterized by 5,6 or 6,6 fused bicyclic ring systems,² which include a pyrimidine or analogue as a core structure (Fig. 2). On the other hand, it was not clear whether a 7,6 fused bicyclic ring system could function effectively as a hinge binder for the HER2 or EGFR proteins.

Molecular modeling studies based on HER2 and EGFR co-crystal structures^{3,4} with TAK-285 suggested that a pyrimido[4,5-*b*]azepine scaffold would fit into the ATP-binding site of the HER2/EGFR protein (Fig. 3). Our analysis suggested that in a manner similar to TAK-285, introduction of a phenoxy anilino group at the C-4 position could occupy a lipophilic back pocket of the HER2 protein. Furthermore, since the pyrimido[4,5-*b*]azepine system has an NH group at the N-9 position, we envisioned that an additional hydrogen bonding interaction could be made with Met801 (HER2)/Met793 (EGFR) in the hinge region to enhance kinase inhibitory

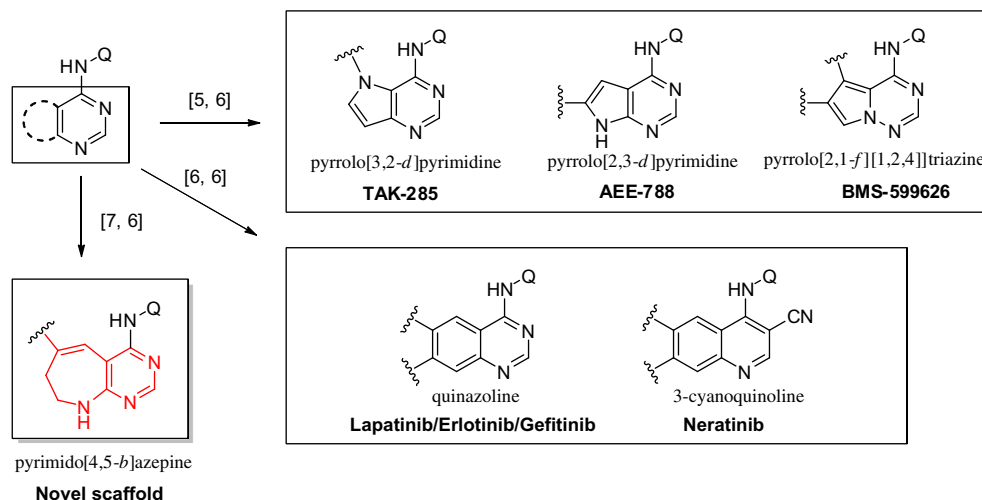


Figure 2. The pyrimido[4,5-*b*]azepine scaffold as a potential alternative for HER2/EGFR kinase inhibition.

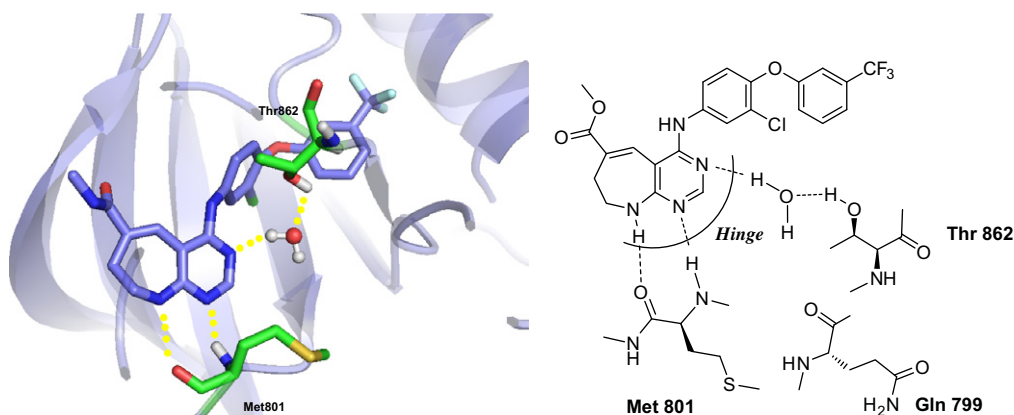


Figure 3. Docking model of a pyrimido[4,5-*b*]azepine derivative **1a** with HER2 protein.

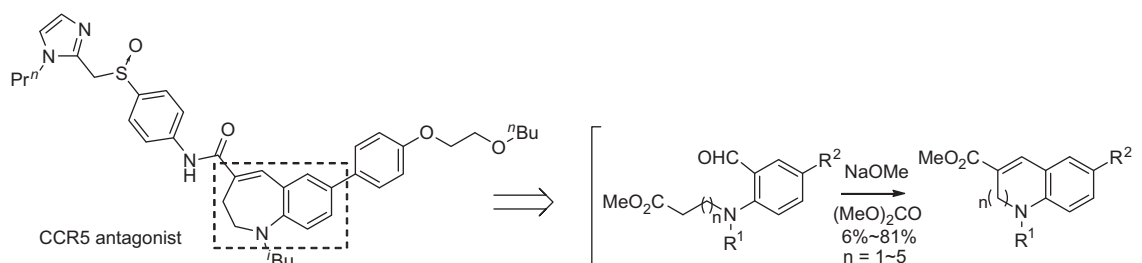
activity. Although the azepine ring is nonaromatic, we confirmed that planarity for the key interactions with HER2 should be maintained. In addition, because the side chain at the C-6 position is directed toward the solvent contact region, we reasoned that chemical modification of the C-6 substituent (*R*) could be utilized to enhance kinase and cell growth inhibitory activity based on an additional hydrogen bond network with amino acid residues around the solvent contact region.

In this paper, we describe the design and structure–activity relationships (SAR) of pyrimido[4,5-*b*]azepine derivatives as well as the development of an effective synthetic route. Crystallographic studies also demonstrated key molecular interactions of the pyrimido[4,5-*b*]azepine scaffold with EGFR.

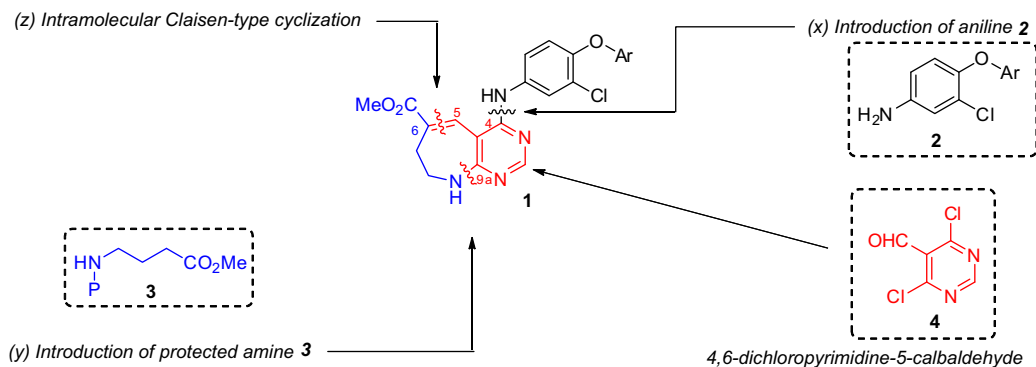
2. Chemistry

To construct the novel pyrimido[4,5-*b*]azepine scaffold, we utilized a reported facile synthesis for 7–10 membered bicyclic fused rings, which were developed for C–C chemokine receptor type 5 (CCR5) antagonists in our laboratories.⁵ The key reaction was an intramolecular Claisen-type condensation by using sodium methoxide and dimethylcarbonate (Scheme 1).

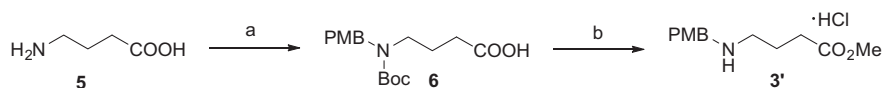
Our synthetic strategy is illustrated in Scheme 2. The designed pyrimido[4,5-*b*]azepine **1** was disconnected into three fragments, which include a phenoxy aniline **2**, 4-(*N*-protected amino)butyric ester **3** and commercially available 4,6-dichloropyrimidine-5-carbaldehyde **4**. We decided that ester **3** could be prepared easily from



Scheme 1. Facile synthesis of 7–10 membered rings by intramolecular Claisen-type condensation.



Scheme 2. Retro-synthesis of pyrimido[4,5-*b*]azepine derivatives.



^a Reagents: (a) (i) 4-methoxybenzaldehyde, Pd/C, H₂, 1*N* NaOH, (ii) Boc₂O, 1*N* NaOH; (b) SOCl₂, MeOH, 61% from **5**.

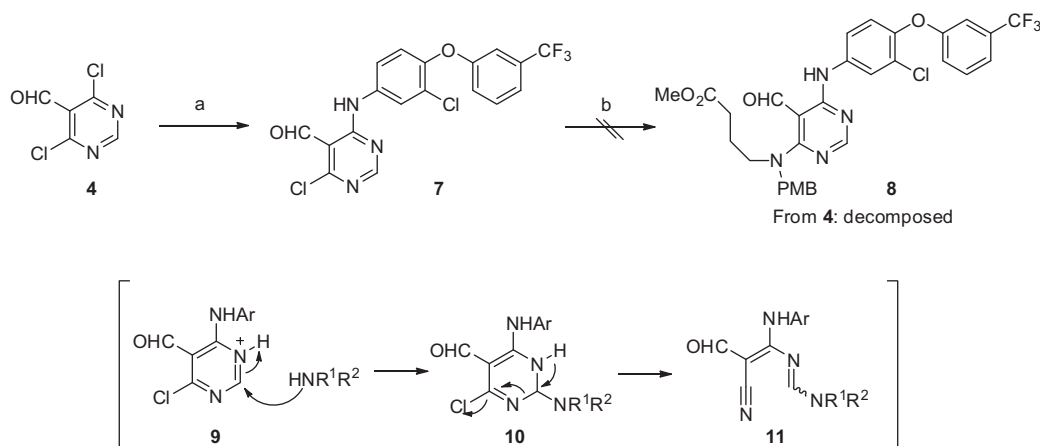
Scheme 3. Synthesis of protected amine **3'**.

commercially available 4-aminobutyric acid. In addition, 3-chloro-4-(3-(trifluoromethyl)phenoxy)aniline **2a** was selected as our representative phenoxy aniline, which is a back pocket binder unit of TAK-285. Next, we explored the synthetic steps necessary to construct the pyrimido[4,5-*b*]azepine scaffold: (x) introduction of aniline **2** at the C-4 position, (y) reaction of protected amine **3** at the C-9a position, and (z) cyclization by intramolecular Claisen-type condensation to make a C=C double bond at the C-5 and C-6 positions.

Synthesis of 4-[(4-methoxybenzyl)amino]butyric ester **3'** is shown in **Scheme 3**. Reductive amination of 4-aminobutyric acid (**5**) with 4-methoxybenzaldehyde in the presence of palladium on carbon (Pd/C) under hydrogen atmosphere followed by introduction of a *tert*-butoxycarbonyl (Boc) group provided Boc-protected acid **6**. Subsequent treatment of **6** with thionyl chloride and methanol afforded the 4-[(4-methoxybenzyl)amino]butyric ester (PMB aminobutyric ester) **3'** as a hydrochloride salt in 61% yield from **5**.

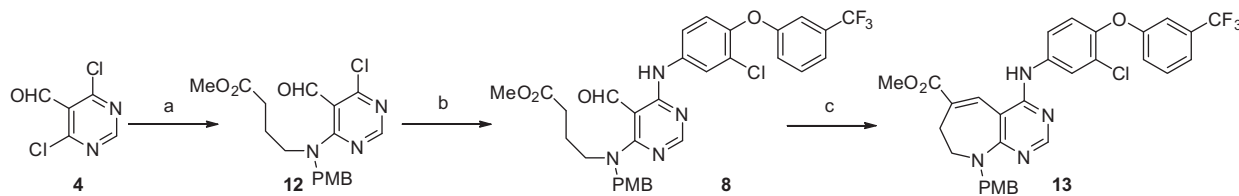
Next, we examined the synthesis of a di-substituted pyrimidine derivative **8** starting from **4**, in particular key steps (x) and (y). We thought that the two reactive chloro groups on the pyrimidine ring of **4** should be substituted before the key cyclization step (z). Thus, we initiated synthetic tests of '(x) then (y)' and '(y) then (x)' to provide precursor **8** for the cyclization step (z). An initial attempt at Route '(x) then (y)' was performed by the reaction of **4** with aniline **2a** to give the corresponding 4-amino pyrimidine **7** (**Scheme 4**). However, the subsequent nucleophilic substitution reaction (y) of **7** with **3'** was unsuccessful and resulted in decomposition of **7**. It has been reported that 6-chloropyrimidine-5-carbaldehyde derivative **9** reacts with nucleophilic amines to provide compounds of type **11**.⁶ Considering the low chemical stability of **7**, we discontinued this synthetic approach.

As an alternative, Route '(y) then (x)', was carried out by reaction of **4** with **3'** to provide the corresponding 6-amino-4-chloropyrimidine derivative **12** in 83% yield. Nucleophilic substitution of **12** with aniline **2a** in the presence of sodium carbonate in



^a Reagents: (a) aniline **2a**, K₃PO₄, MeCN; (b) **3'**, Na₂CO₃, DMF.

Scheme 4. Synthetic approach to cyclization precursor **8** (Route "(x) then (y)").



^a Reagents: (a) **3'**, K₃PO₄, MeCN, rt, 21 h, 83%; (b) aniline **2a**, Na₂CO₃, DMF, 60 °C, 108 h; (c) dimethyl carbonate, 28% sodium methoxide-methanol solution, rt, 15 h, 47% from **12**.

Scheme 5. Synthetic approach to cyclization precursor **8** (Route “(y) then (x)”) to provide pyrimido[4,5-*b*]azepine derivative **13**.

N,N-dimethylformamide (DMF) at 60 °C afforded the desired precursor **8**. Subsequent Claisen-type cyclization of the resulting **8** with sodium methoxide and dimethylcarbonate provided the desired PMB protected pyrimido[4,5-*b*]azepine derivative **13** in 47% yield in 2 steps from **12** (Scheme 5). However, lengthy reaction time (108 h) was required to complete the second nucleophilic substitution reaction of **12**. Heating the reaction mixture in acetonitrile at 80 °C resulted in decomposition of **12** similar to that observed for Route “(x) then (y)”.

As a result of these unsuccessful results, we switched our synthetic route to the early formation of the pyrimido[4,5-*b*]azepine scaffold according to Route “(y), (z), (x)” as shown in Schemes 6 and 7. For this purpose, the 4-chloropyrimidine derivative **12** was used as a starting material, although the possibility of undesired side reactions was thought to exist based on the high reactivity of the pyrimidine 4-chloro group. As predicted, undesired side reaction occurred in the cyclization step using sodium methoxide and dimethylcarbonate to provide the C-4 methoxy substituted pyrimido[4,5-*b*]azepine derivative **14** in 88% yield. Fortunately, after removal of the PMB protective group with trifluoroacetic acid (TFA) in 91% yield, the pyrimido[4,5-*b*]azepine **15** thus obtained was efficiently converted into the desired 4-chloropyrimido[4,5-*b*]azepine intermediate **16** by reaction with phosphoryl chloride in 92% yield. Hydrolysis of ester **16** with 6 N HCl followed by crystallization produced carboxylic acid **17** as a hydrochloride salt in 69% yield. From these results, this Route “(y), (z), (x)” was selected as our standard method for the synthesis of pyrimido[4,5-*b*]azepine derivatives.

Pyrimido[4,5-*b*]azepine derivative **17** was characterized by ¹H NMR and single crystal X-ray analysis. X-ray analysis of **17** revealed that the pyrimido[4,5-*b*]azepine ring retains its co-planarity between the pyrimidine and azepine rings without apparent strain

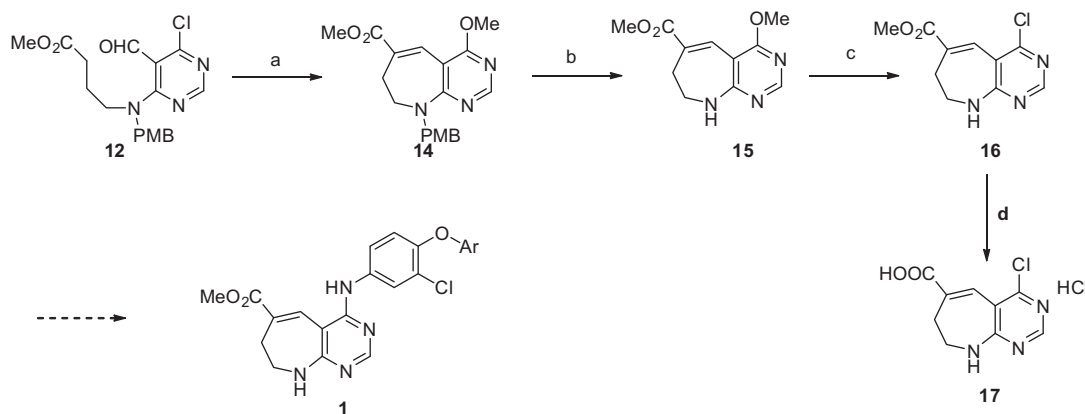
(Fig. 4). Since a common structure of kinase hinge binders, including 5,6- or 6,6-bicyclic fused ring systems, is a planar aromatic fused ring, this co-planarity of the pyrimido[4,5-*b*]azepine ring should contribute to interact effectively with HER2/EGFR proteins similarly to other bicyclic inhibitors.

The establishment of a facile synthetic route to key intermediate **16** accelerated our research toward the optimization of both C-4 aniline and C-6 substituents. On the basis of our previous studies of pyrrolo[3,2-*d*]pyrimidine compounds,³ we selected another C-4 aniline, 4-(benzo[*b*]thiophen-4-yloxy)-3-chloroaniline (**2b**) to be employed in the synthesis of pyrimido[4,5-*b*]azepine derivatives possessing potent HER2/EGFR inhibitory activity as well as cellular growth inhibitory (GI) potency. In our previous report,⁷ we proposed an intereaction between the sulfur atom on 1-benzothiophene ring with C=O groups on the Ser783/Cys775 residues of HER2/EGFR, and the derivatives prepared showed good cellular GI activity as a result of their observed pseudo-irreversibility (PI).

The synthesis of 4,6-substituted pyrimido[4,5-*b*]azepine derivatives **19** and **20** is shown in Scheme 7. Condensation of **16** with aniline **2a** or **2b** in 2-propanol (73% and 91% yield), followed by hydrolysis of the methyl ester in **1a,b** with sodium hydroxide to afford key intermediates **18a,b** in 86% and 96% yield, respectively. Condensation of **18a,b** with several amines in the presence of 1-ethyl-3-(3-dimethylaminopropyl)carbodiimide hydrochloride (EDC) and 1-hydroxybenzotriazole monohydrate (HOBt) provided the corresponding carboxamides (**19, 20**) in 40–77% yield.

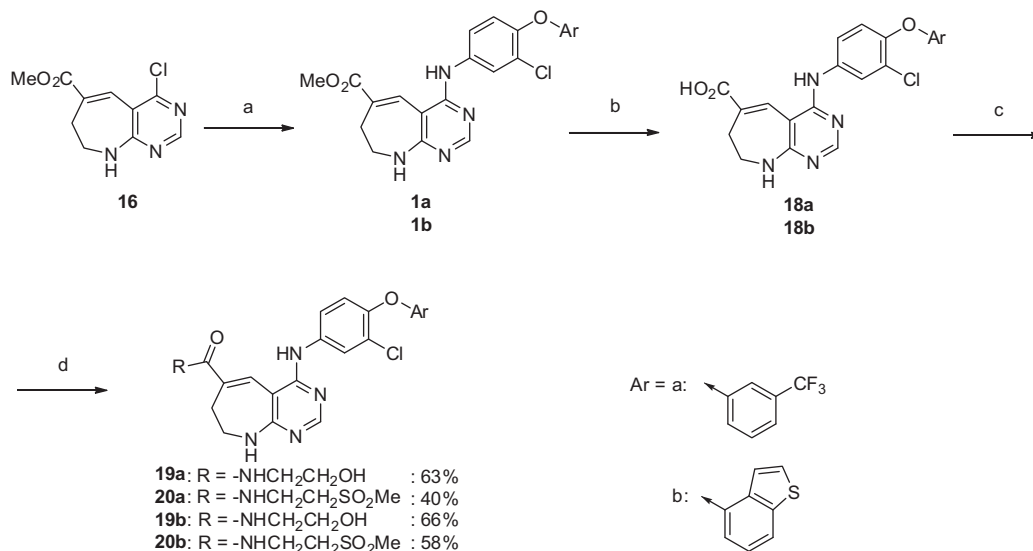
3. Results and discussion

To examine the potential of the pyrimido[4,5-*b*]azepine scaffold for use in the discovery of HER2/EGFR kinase inhibitors, derivatives **1, 19** and **20** were evaluated in depth. Table 1 shows their



^a Reagents: (a); NaOMe, (MeO)₂CO, 88%; (b) TFA, Toluene, 91%; (c) POCl₃, 92%; (d) 6N HCl, MeOH, 69%.

Scheme 6. Synthesis of the pyrimido[4,5-*b*]azepine scaffold (Route “(y) then (z) then (x)”).



^a Reagents: (a) aniline **2a** or **2b**, 2-propanol, 73% and 91%; (b) 1*N* NaOH, MeOH, THF, 86% and 96%; (c) amine, EDC, HOBT, Et₃N, THF, DMF

Scheme 7. Synthesis of pyrimido[4,5-*b*]azepine derivatives (Route “(y), (z), (x)”).

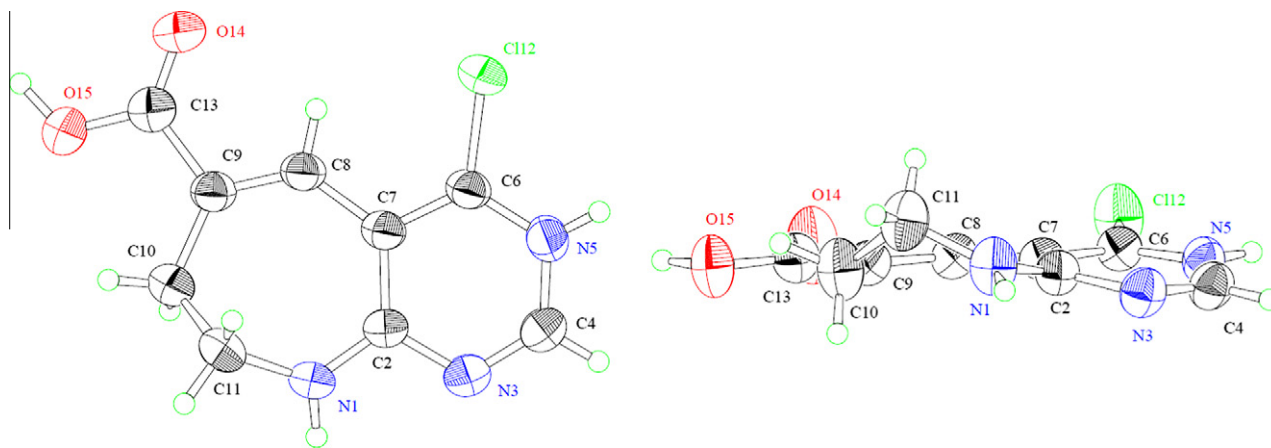


Figure 4. Single-crystal X-ray structure of **17**.

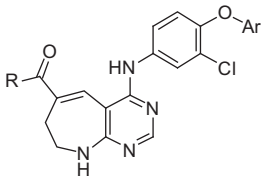
HER2/EGFR kinase and tumor cell growth (BT-474, a HER2-over-expressing human breast cancer cell line) inhibitory activities. Almost all of the derivatives showed potent HER2/EGFR inhibitory activities with IC₅₀ values less than 100 nM, especially against HER2. These results suggested that the N-1/N-3 nitrogen atoms of the pyrimido[4,5-*b*]azepine scaffold can interact with the Met801 and Thr862 residues in the hinge region of the HER2 ATP-binding pocket and that the 4-anilino group fits into the lipophilic back pocket as predicted from our structural data. Among these 3-trifluoromethylphenoxy derivatives (**1a**, **19a**, **20a**), **19a** showed the most potent HER2/EGFR inhibitory activity, which revealed that the chemical modification of the side chain at the C-6 position was effective at enhancing kinase inhibitory activity. However, **19a** exhibited moderate cell growth inhibitory (GI) activity against BT-474 cell line with a GI₅₀ value of 630 nM (TAK-285, GI₅₀ 17 nM). On the other hand, the 1-benzothiophene derivatives (**1b**, **19b**, **20b**) each showed not only more potent HER2/EGFR inhibitory activity but also significantly more potent cell GI activity than the corresponding 3-trifluoromethylphenoxy derivatives **1a**, **19a** and **20a**.

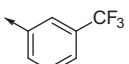
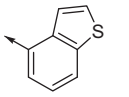
Considering our previous research on the exploration of back pocket binding moieties,⁷ we proposed that replacement of the 3-trifluoromethylphenoxy group with the 1-benzothiophen-4-yloxy moiety on the anilino group could enhance their PI profiles. In Figure 5, the dissociation rates of compound **19b** from HER2 and EGFR in a 100-fold dilution assay^{7,8} are presented compared with those for TAK-285. As expected, compound **19b** showed strong PI effects for both HER2 and EGFR kinases and was shown to have a characteristic slow-off rate profile.

The inhibitory activities of **19b** against various kinases are listed in Table 2. Besides HER2 and EGFR, **19b** exhibited HER4, B-raf (wild type) and MEK5 inhibitory activities with IC₅₀ values of 240, 230 and 870 nM. Since our previous scaffold pyrrolo[3,2-*d*]pyrimidine did not show significant inhibitory activity against B-raf (wild type) and MEK5,³ transformation of the 5,6- to a 7,6-fused bicyclic ring system or the presence of NH group at the pyrimido[4,5-*b*]azepine 9-position may affect its kinase selectivity.

We determined crystal structures of EGFR bound to compounds **19b** and **20a** to better understand the structure–activity relationships observed. Both compounds are bound to the ATP binding site

Table 1
Biological profiles for pyrimido[4,5-*b*]azepine derivatives



Compd	R	Ar	Enzyme IC ₅₀ (nM)		Cell growth GI ₅₀ (nM)
			HER2	EGFR	BT-474
1a	-OMe		100	110	2000
19a	-NHCH ₂ CH ₂ OH		29	38	630
20a	-NHCH ₂ CH ₂ SO ₂ Me		65	75	620
1a	-OMe		18	44	190
19a	-NHCH ₂ CH ₂ OH		24	36	18
20a	-NHCH ₂ CH ₂ SO ₂ Me		30	47	25
TAK-285			17	23	17

These measurements are described in experimental section. IC₅₀ values were calculated by nonlinear regression analysis of the percentage inhibitions ($n = 2$). HER2 over-expressing human cancer cell (BT-474) was used for the cell growth assays. The cells were treated continuously with compounds for 5 days and then the live cell numbers were counted with a particle analyzer (CDA-500; Sysmex Corporation) to determine GI₅₀ values.

in the predicted binding mode and the pyrimido[4,5-*b*]azepine scaffold forms three major hydrogen-bond interactions with EGFR. The N-1 and N-9 nitrogens of **20a** make hydrogen bonds with the main-chain nitrogen and oxygen of the hinge region Met793, respectively (Fig. 6A). In addition, the N-3 nitrogen forms a water-mediated hydrogen bond with the side chain of Thr854. Furthermore, the aniline nitrogen at the C-4 position and the carboxamide NH of the C-6 side chain form a water-mediated intramolecular hydrogen bond network. The intramolecular hydrogen bond network may play an important role in adapting to provide a suitable angle between the C-6 side chain and the C-4 anilino moiety. This would explain why replacement of the C-6 ester group (**1a**) with the carboxamide group (**19a**) is effective in enhancing HER2/EGFR kinase inhibitory activity. In comparison with the single-crystal structure of **17**, the conformation of the azepine ring in the complex with EGFR is subtly distorted due to steric repulsion between the C-7 carbon atom of the pyrimido[4,5-*b*]azepine ring and the side chain of Leu718 (Fig. 6B).

A comparison of the crystal structures of EGFR complexed with compound **20a** or with TAK-285 revealed that the amide oxygen at the N-5 position of TAK-285 is located in the same position as the water bridging the C-4 aniline nitrogen and the C-6 side chain carboxamide NH for compound **20a**. This amide oxygen makes a direct intramolecular hydrogen bond with the aniline nitrogen at the C-4 position, whereas the direct interaction of N-1 with the hinge region and the water-mediated interaction of N-3 with Thr854 are remarkably conserved between the two structures (Fig. 6C). The conformational preference of substituents relative to the scaffold may be critical for proper spatial configuration in the binding site. The trifluoromethyl-phenoxy group occupies a hydrophobic environment in the vicinity of the DFG motif and α C helix in the same binding mode. No significant conformational differences for the EGFR protein were observed except for disordered surface regions of the EGFR/TAK-285 complex. Notably, the activation loop is well ordered and forms two short helical segments in the EGFR/**20a** complex (data not shown). To our knowledge, this is the first such observation for EGFR, which may provide a structural basis for understanding activation mechanism of EGFR. These results could rationalize the slightly lower potency of the pyrimido[4,5-*b*]azepine derivative against EGFR relative to the corresponding pyrrolo[3,2-*d*]pyrimidine derivative (Table 1).³

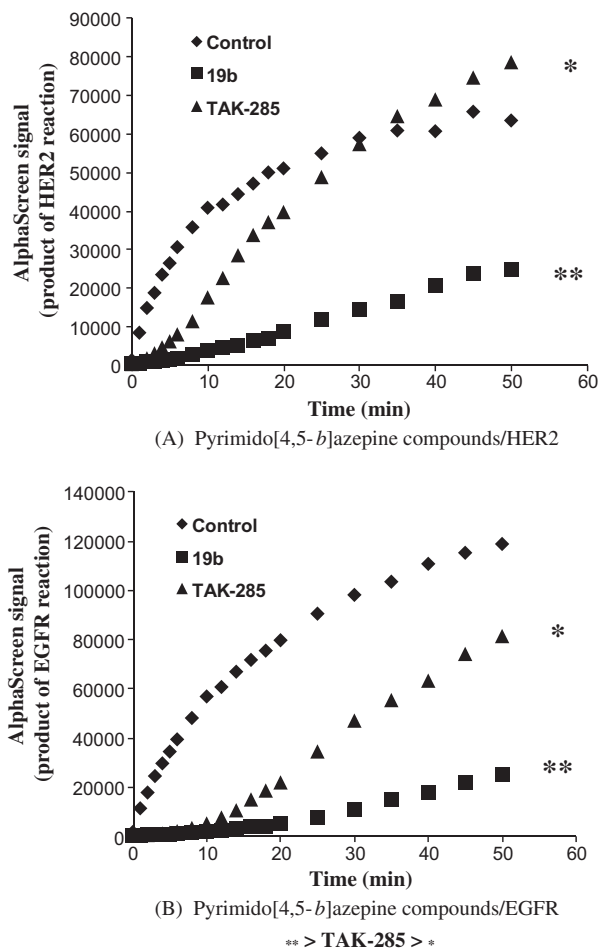


Figure 5. Dissociation of pyrimido[4,5-*b*]azepine compounds from EGFR (A) and HER2 (B). Phosphorylation of peptide substrate as a function of time is shown. The reaction was initiated by diluting a preformed enzyme-inhibitor complex into reaction buffer. To determine the dissociation kinetics of the inhibitors from HER2 and EGFR, the recovery of enzyme activity from a preformed enzyme-inhibitor complex was evaluated using the Alphascreen® system (PerkinElmer, USA). The PI strengths of compounds, compared with **1**, are indicated by 2 asterisks (**) when the compounds showed obviously strong PI profiles, and by a single asterisk (*) when PI was weak compared with that of TAK-285.

Table 2
Kinase selectivity of **19b**, IC₅₀ (nM)

HER2	24	B-raf wild	230	LYNB	3000	LYNA	9800
EGFR	36	MEK5	870	LCK	3200	Other 28 Kinases ^a	>10,000
HER4	240	P38a	1700	c-mey	5600		

^a Other kinases: c-kit, AuroraB, MEK1, TIE2, FGFR1, FGFR3, ASK1, CSK, FAK, MEKK, VEGFR1, VEGFR2, PDGFRa, PDGFRb, TTK, TAK1, PLK, PKCtheta, PKA, BMX, IGF1-R, InsR, ZAP70, ERK1, GSK3b, IKK, JNK, Src.

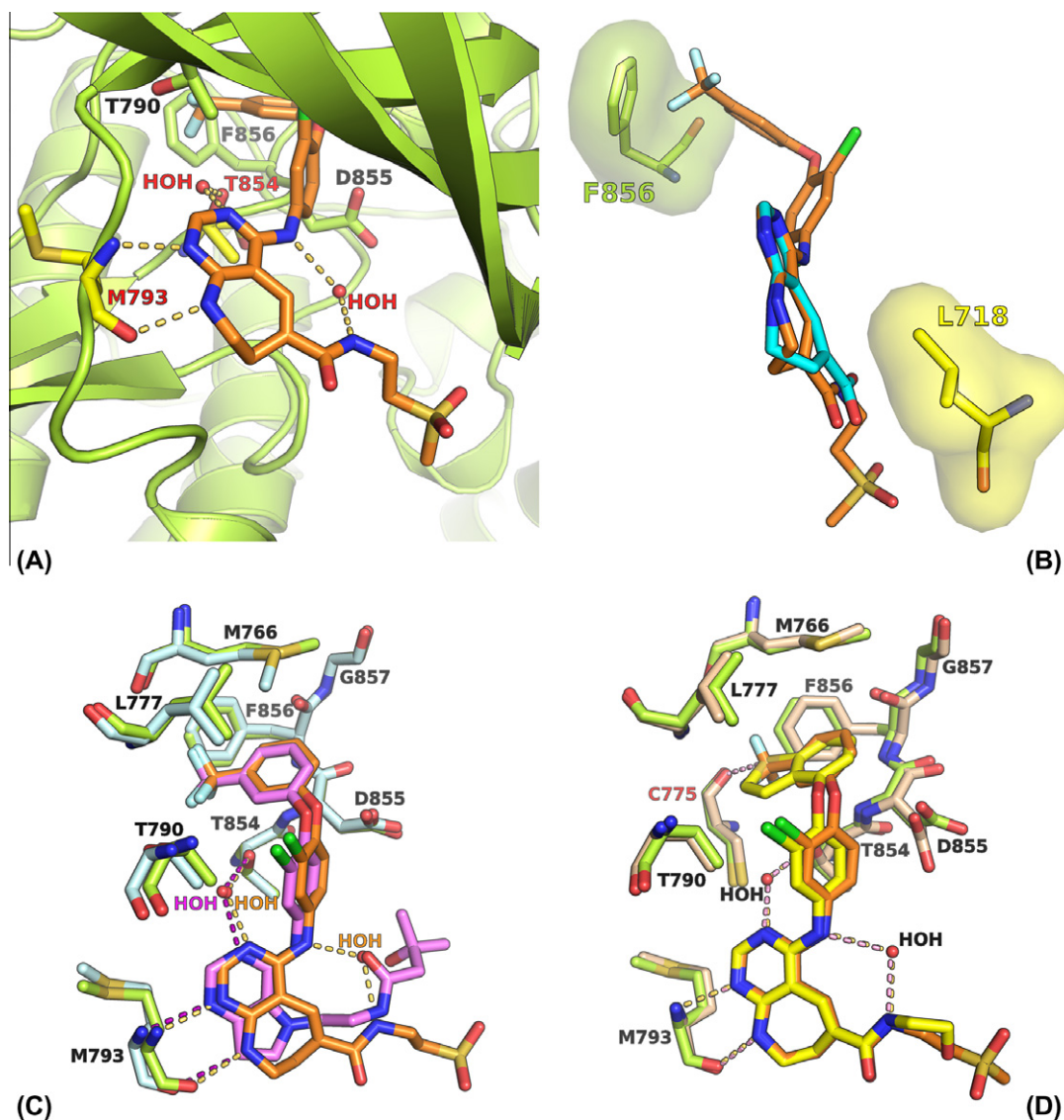


Figure 6. Crystal structures of EGFR. (A) The complex with **20a** (orange), (B) Superposition of **17** (cyan) onto **20a** (orange). (C) Comparison of **20a** (orange) with TAK-285 (violet). Water molecules of each structure are labeled in the same color. (D) Comparison of **20a** (orange) with **19b** (yellow). Cys775 is labeled in red.

The crystal structure of the EGFR/**19b** complex was superposed onto that of the EGFR/**20a** complex to shed light on their distinct PI profiles, which may correlate with cell-growth inhibition. The benzothiazepine ring of **19b** occupies the hydrophobic pocket in a similar manner to the trifluoromethyl-phenyl group of **20a** with nearly equivalent enzyme inhibition (Fig. 6D). The sulfur atom of the benzothiazepine ring interacts with the main-chain oxygen of Cys775. No distinct conformational rearrangement upon inhibitor binding was observed in the hydrophobic pocket involving the N-lobe segment, the α C helix, the DFG motif and the activation loop. Taken together, these results suggest that the key interactions and the proper steric bulkiness of the benzothiazepine ring could facilitate accommodation of the inactive conformation and lead a long resi-

dence time of **19b** on EGFR, resulting in the enhancement of PI behavior. However, a complete understanding of the relation between these structural and cell-growth inhibition data remains elusive. Further investigation will enable us to better understand the SAR for these compounds.

4. Conclusion

We designed a novel 7,6-fused bicyclic pyrimido[4,5-*b*]azepine scaffold to fit into the ATP binding site of the HER2/EGFR proteins. The synthesis of this scaffold has been accomplished by intramolecular Claisen-type condensation and further studies afforded an efficient synthetic route via an important key intermediate,

4-chloropyrimido[4,5-*b*]azepine **16**. Representative pyrimido[4,5-*b*]azepine derivative **19b**, bearing the 1-benzothiophen-4-yloxy group as a back pocket binding moiety, showed potent HER2/EGFR kinase (IC₅₀: 24/36 nM) and BT474 cell growth (GI₅₀: 18 nM) inhibitory activities as a result of its strong PI behavior. X-ray co-crystal structural analysis of **19b** and **20a** bound to EGFR also showed that the pyrimido[4,5-*b*]azepine scaffold interacts effectively with the EGFR protein. These results provide new insights into novel HER2/EGFR kinase inhibitors.

5. Experimental

Melting points were determined on a Yanagimoto micro melting point apparatus or SRS OptiMelt melting point apparatus, and are uncorrected. Proton nuclear magnetic resonance (¹H NMR) spectra were recorded on a Varian Gemini-200 (200 MHz) spectrometer or Varian Mercury-300 (300 MHz) spectrometer. Chemical shifts are given in parts per million (ppm) with tetramethylsilane as an internal standard, and coupling constants (*J* values) are given in Hertz (Hz). Splitting patterns and apparent multiplicities are designated as s (singlet), d (doublet), dd (double doublet), t (triplet), dt (double triplet), q (quartet), m (multiplet), br s (broad singlet). Elemental analyses were carried out by Takeda Analytical Research Laboratories, Ltd, and the results obtained were within ±0.4% of the theoretical values. MS spectra were collected with a Waters LC-MS system (ZMD-1) and were used to confirm ≥95% purity of each compound. The column used was an L-column 2 ODS (3.0 × 50 mm I.D., CERI, Japan) with a temperature of 40 °C and a flow rate of 1.2 mL/min. Mobile phase A was 0.05% TFA in ultrapure water. Mobile phase B was 0.05% TFA in acetonitrile which was increased linearly from 5% to 90% over 2 min, 90% over the next 1.5 min, after which the column was equilibrated to 5% for 0.5 min. Column chromatography was carried out on a silica gel column (Kieselgel 60, 63–200 mesh, Merck or Chromatorex[®] NH-DM1020, 100–200 mesh, Fuji Silysia chemical). Yields were not optimized.

Commercial reagents and solvents were used without additional purification. Abbreviations are used as follows: CDCl₃, deuterated chloroform; DMSO-*d*₆, dimethyl sulfoxide-*d*₆; AcOEt, ethyl acetate; DMF, *N,N*-dimethylformamide; MeOH, methanol; THF, tetrahydrofuran; EtOH, ethanol; DMSO, dimethyl sulfoxide; NMP, *N*-methylpyrrolidone.

5.1. Methyl 4-((4-methoxybenzyl)amino)butanoate hydrochloride (**3'**)

To a solution of 4-aminobutyric acid (**5**) (20.6 g, 20.0 mmol), 1 N NaOH (200 mL) and 4-methoxybenzaldehyde (29.9 g, 20.0 mmol) in EtOH (300 mL) was added 10% palladium-carbon (Pd/C) (4.0 g), and the reaction mixture was stirred at room temperature under hydrogen atmosphere for 7 days. The insoluble 10% Pt/C was filtered off and the filtrate was concentrated in vacuo. To the residue, THF (200 mL) and di-*tert*-butyl dicarbonate (Boc₂O) (43.0 g, 0.197 mol) were added at room temperature. After being stirred at room temperature for 3 h, the mixture was extracted with hexane (200 mL). To the aqueous layer was added 1 N HCl until pH 2 and extracted with diethyl ether (Et₂O) (200 mL). The combined organic layers were washed with saturated brine (15 mL), dried over MgSO₄, and concentrated in vacuo. The residue was dissolved in MeOH (240 mL) and then to the mixture was added dropwise thionyl chloride (47 mL, 0.644 mol) at –10 °C. The mixture was stirred at room temperature for 24 h and concentrated in vacuo. The residual solid was washed with Et₂O (100 mL) to give 42.0 g (89%) of **3'** as a white powder. ¹H NMR (DMSO-*d*₆) δ 1.82–1.96 (2H, m), 2.44 (2H, t, *J* = 7.4 Hz), 2.80–2.92 (2H, m), 3.60 (3H, s), 3.77 (3H, s), 4.04 (2H, t, *J* = 5.7 Hz), 6.98 (2H, d, *J* = 8.7 Hz), 7.47 (2H, d, *J* = 8.7 Hz), 9.08–9.25 (2H, m).

5.2. Methyl 4-((6-chloro-5-formylpyrimidin-4-yl)(4-methoxybenzyl)amino)butanoate (**12**)

To a solution of 4,6-dichloropyrimidine-5-carbaldehyde (7.75 g, 43.8 mmol) in acetonitrile (780 mL) were added potassium phosphate (20.5 g, 96.4 mmol) and **3'** (12.0 g, 43.8 mmol), and the mixture was stirred at room temperature for 15.5 h. The reaction mixture was concentrated in vacuo. To the residue was added water, and the mixture was extracted with EtOAc (200 mL). The organic layer was washed with saturated brine (20 mL), dried over MgSO₄, and concentrated in vacuo. The residue was purified by silica gel column chromatography (5–33% EtOAc/hexane eluent) to give 13.8 g (83%) of **12** as a yellow oil. ¹H NMR (CDCl₃) δ 1.89–2.02 (2H, m), 2.31 (2H, t, *J* = 7.3 Hz), 3.60–3.68 (2H, m), 3.65 (3H, s), 3.79 (3H, s), 4.56 (2H, s), 6.83 (2H, d, *J* = 8.8 Hz), 7.01 (2H, d, *J* = 8.5 Hz), 8.39 (1H, s), 10.19 (1H, s).

5.3. Methyl 4-((3-chloro-4-(3-(trifluoromethyl)phenoxy)phenyl)amino)-9-(4-methoxybenzyl)-8,9-dihydro-7H-pyrimido[4,5-*b*]azepine-6-carboxylate (**13**)

To a solution of **12** (11.0 g, 29.1 mmol) in DMF (110 mL) were added sodium carbonate (3.10 g, 22.4 mmol) and 3-chloro-4-[3-(trifluoromethyl)phenoxy]aniline³ (8.39 g, 29.1 mmol), and the mixture was stirred at 60 °C for 108 h. To the reaction mixture was added water (400 mL), and the mixture was extracted with EtOAc (300 mL). The organic layer was washed with saturated brine (20 mL), dried over MgSO₄, and concentrated in vacuo. The residue was purified by silica gel column chromatography (eluent, EtOAc/hexane = 10:90 to 50:50). The obtained oil was dissolved in dimethyl carbonate (230 mL). To the solution was added 28% sodium methoxide/MeOH solution (12.3 g, 63.6 mmol) and the mixture was stirred at room temperature for 15 h. The reaction mixture was neutralized by 1 N HCl and extracted with EtOAc (400 mL). The organic layer was washed with saturated brine (20 mL), dried over MgSO₄, and concentrated in vacuo. The residue was purified by basic silica gel column chromatography (eluent, EtOAc/hexane = 10:90 to 50:50) to give 8.44 g (47%) of **13** as a yellow oil. ¹H NMR (CDCl₃) δ 2.66 (2H, t, *J* = 4.6 Hz), 3.30–3.40 (2H, m), 3.78 (3H, s), 3.81 (3H, s), 4.87 (2H, s), 6.81–6.91 (3H, m), 7.03–7.14 (2H, m), 7.19–7.29 (3H, m), 7.30–7.36 (1H, m), 7.37–7.47 (2H, m), 7.68 (1H, s), 7.75 (1H, d, *J* = 2.7 Hz), 8.24 (1H, s).

5.4. Methyl 4-methoxy-9-(4-methoxybenzyl)-8,9-dihydro-7H-pyrimido[4,5-*b*]azepine-6-carboxylate (**14**)

To a solution of **12** (15.4 g, 40.8 mmol) in dimethyl carbonate (150 mL) was added 28% sodium methoxide/MeOH solution (23.6 g, 122 mmol) at room temperature. The mixture was stirred at room temperature for 24 h. To the reaction mixture was added water (200 mL), and the mixture was extracted with EtOAc (150 mL). The organic layer was washed with saturated brine (15 mL), dried over MgSO₄, and concentrated in vacuo. The residue was purified by silica gel column chromatography (eluent, EtOAc/hexane = 33:67 to 50:50) to give 12.8 g (88%) of **14** as a white solid. ¹H NMR (CDCl₃) δ 2.66–2.70 (2H, m), 3.28–3.32 (2H, m), 3.78 (3H, s), 3.79 (3H, s), 4.03 (3H, s), 4.88 (2H, s), 6.85 (2H, d, *J* = 8.7 Hz), 7.19 (2H, d, *J* = 8.7 Hz), 8.09 (1H, t, *J* = 1.2 Hz), 8.24 (1H, s).

5.5. Methyl 4-methoxy-8,9-dihydro-7H-pyrimido[4,5-*b*]azepine-6-carboxylate (**15**)

To a solution of **14** (476 mg, 1.34 mmol) in toluene (5.0 mL) was added trifluoroacetic acid (2.5 mL) at room temperature. The mixture was stirred at 70 °C for 20 h and concentrated in vacuo. To the

residue was added saturated sodium hydrogen carbonate (20 mL), and extracted with EtOAc (40 mL). The organic layer was washed with saturated brine (5 mL), dried over MgSO₄, and concentrated in vacuo. The precipitated solid was collected by filtration and washed with diisopropyl ether (20 mL) to give 288 mg (91%) of **15** as a white solid. ¹H NMR (CDCl₃) δ 2.89 (2H, t, *J* = 4.5 Hz), 3.46 (2H, q, *J* = 4.5 Hz), 3.80 (3H, s), 4.01 (3H, s), 5.79–5.87 (1H, m), 8.04 (1H, d, *J* = 1.2 Hz), 8.12 (1H, s).

5.6. Methyl 4-chloro-8,9-dihydro-7H-pyrimido[4,5-*b*]azepine-6-carboxylate (**16**)

A mixture of **15** (2.55 g, 10.8 mmol) and phosphoryl chloride (26 mL) was stirred at 100 °C for 96 h. The reaction mixture was concentrated in vacuo, and ice was added to the residue at 0 °C. The mixture was neutralized with saturated aqueous ammonia. The precipitated solid was collected by filtration and washed with water (20 mL) to give **16** (2.40 g, 92%) as a pale yellow powder. ¹H NMR (CDCl₃) δ 2.88–2.98 (2H, m), 3.46–3.57 (2H, m), 3.84 (3H, s), 6.18 (1H, br s), 8.14 (1H, s), 8.20 (1H, s).

5.7. 4-Chloro-8,9-dihydro-7H-pyrimido[4,5-*b*]azepine-6-carboxylic acid hydrochloride (**17**)

A mixture of **16** (100 mg, 0.42 mmol), 6 N HCl (1.20 mL, 1.20 mmol) and MeOH (2 mL) was stirred at 60 °C for 1 h. After cooling at room temperature, the obtained crystals were collected by filtration to give **17** (75 mg, 69%) as colorless crystals. Mp 162–164 °C. ¹H NMR (DMSO-*d*₆) δ 2.63–2.85 (2H, m), 3.35 (2H, q, *J* = 4.5 Hz), 7.96 (1H, s), 8.63 (1H, br s).

5.8. Methyl 4-((3-chloro-4-(3-(trifluoromethyl)phenoxy)phenyl)amino)-8,9-dihydro-7H-pyrimido[4,5-*b*]azepine-6-carboxylate (**1a**)

A solution of pyridinium chloride (82.7 mg, 0.716 mmol), **16** (1.76 g, 7.34 mmol) and 3-chloro-4-(3-(trifluoromethyl)phenoxy)aniline (**2a**, 2.28 g, 7.93 mmol) in 2-propanol (40 mL) was stirred at 90 °C for 14 h. After cooling at room temperature, the reaction mixture was quenched with saturated sodium hydrogen carbonate (20 mL), and extracted with EtOAc (40 mL). The organic layer was washed with saturated brine (10 mL), dried over MgSO₄ and concentrated in vacuo. The residue was purified by silica gel column chromatography (eluent, EtOAc/hexane = 10:90 to 80:20) to give **1a** (2.36 g, 66%) as white crystals. Mp 197–199 °C. ¹H NMR (CDCl₃) δ 2.86–2.94 (2H, m), 3.53 (2H, q, *J* = 4.3 Hz), 3.82 (3H, s), 5.86 (1H, t, *J* = 4.3 Hz), 6.88 (1H, s), 7.06 (1H, d, *J* = 8.7 Hz), 7.10 (1H, dd, *J* = 8.0, 2.2 Hz), 7.21 (1H, br s), 7.29–7.49 (3H, m), 7.68 (1H, s), 7.75 (1H, d, *J* = 2.6 Hz), 8.13 (1H, s). Anal. Calcd for C₂₃H₁₈ClF₃N₄O₃ · 0.5 H₂O: C, 55.26; H, 3.83; N, 11.21. Found: C, 55.51; H, 3.69; N, 11.35.

5.9. Methyl 4-((4-(benzo[*b*]thiophen-4-yloxy)-3-chlorophenyl)amino)-8,9-dihydro-7H-pyrimido[4,5-*b*]azepine-6-carboxylate (**1b**)

Compound **1b** was obtained as colorless crystals in 91% yield from **16** by a method similar to that described for **1a**. Mp 219–220 °C. ¹H NMR (CDCl₃) δ 2.90 (2H, t, *J* = 4.8 Hz), 3.52 (2H, q, *J* = 4.8 Hz), 3.82 (3H, s), 5.76–5.84 (1H, m), 6.71–6.74 (1H, m), 6.81 (1H, s), 6.97 (1H, d, *J* = 9.0 Hz), 7.22–7.31 (2H, m), 7.41–7.42 (1H, m), 7.50–7.52 (1H, m), 7.62 (1H, d, *J* = 8.1 Hz), 7.66 (1H, s), 7.73 (1H, d, *J* = 2.4 Hz), 8.11 (1H, s). Anal. Calcd for C₂₄H₁₉ClN₄O₃S: C, 60.19; H, 4.00; N, 11.70. Found: C, 59.84; H, 4.17; N, 11.70.

5.10. 4-((3-Chloro-4-(3-(trifluoromethyl)phenoxy)phenyl)amino)-8,9-dihydro-7H-pyrimido[4,5-*b*]azepine-6-carboxylic acid (**18a**)

To a solution of **1a** (2.34 g, 4.78 mmol) in THF (70 mL) and EtOH (70 mL) was added 1 N NaOH (15 mL), and the mixture was stirred at room temperature for 14 h. To the reaction mixture was added 1 N HCl until pH 3, and the mixture was diluted with water (200 mL). The precipitate was filtered and dried to give **18a** (1.96 g, 86%) as a pale yellow solid. ¹H NMR (DMSO-*d*₆) δ 2.65–2.78 (2H, m), 3.19–3.48 (2H, m), 7.13–7.29 (3H, m), 7.45 (1H, d, *J* = 7.7 Hz), 7.51–7.64 (2H, m), 7.71 (1H, s), 7.84 (1H, d, *J* = 2.5 Hz), 7.89 (1H, t, *J* = 4.8 Hz), 7.99 (1H, s), 9.40 (1H, s).

5.11. 4-((4-(Benzo[*b*]thiophen-4-yloxy)-3-chlorophenyl)amino)-8,9-dihydro-7H-pyrimido[4,5-*b*]azepine-6-carboxylic acid (**18b**)

Compound **18b** was obtained as a pale yellow solid in 96% yield from **1b** by a method similar to that described for **18a**. ¹H NMR (DMSO-*d*₆) δ 2.65–2.75 (2H, m), 3.27–3.40 (2H, m), 6.60 (1H, d, *J* = 7.2 Hz), 7.12 (1H, d, *J* = 8.7 Hz), 7.29 (1H, d, *J* = 8.1 Hz), 7.46–7.52 (2H, m), 7.68–7.86 (5H, m), 7.96 (1H, s), 9.34 (1H, s).

5.12. 4-((3-Chloro-4-(3-(trifluoromethyl)phenoxy)phenyl)amino)-*N*-(2-hydroxyethyl)-8,9-dihydro-7H-pyrimido[4,5-*b*]azepine-6-carboxamide (**19a**)

To a solution of **18a** (99.9 mg, 0.210 mmol) in a mixed solvent of THF (0.5 mL) and DMF (0.5 mL) were successively added 2-aminoethanol (0.02 mL, 0.330 mmol), 1-hydroxybenzotriazole (HOBT) (44.3 mg, 0.328 mmol), triethylamine (0.1 mL, 0.717 mmol) and 1-ethyl-3-(3-dimethylaminopropyl)carbodiimide hydrochloride (EDC) (87.3 mg, 0.455 mmol), and the mixture was stirred at room temperature for 2 h. To the reaction mixture was added water (30 mL), and the mixture was extracted with EtOAc (20 mL). The organic layer was washed with saturated brine (5 mL), dried over MgSO₄, and concentrated in vacuo. The residue was purified by silica gel column chromatography (eluent, EtOAc/hexane = 0:100 to 90:10) to give **19a** (68.8 mg, 63%) as white crystals. Mp 163–165 °C. ¹H NMR (DMSO-*d*₆) δ 2.64–2.72 (2H, m), 3.19–3.29 (2H, m), 3.29–3.39 (2H, m), 3.42–3.52 (2H, m), 4.70 (1H, t, *J* = 5.6 Hz), 7.14–7.23 (3H, m), 7.26 (1H, d, *J* = 8.8 Hz), 7.46 (1H, d, *J* = 8.0 Hz), 7.55–7.71 (3H, m), 7.90 (1H, d, *J* = 2.5 Hz), 7.95–8.03 (2H, m), 9.11 (1H, s). Anal. Calcd for C₂₄H₂₁ClF₃N₅O₃ · 0.1H₂O: C, 55.25; H, 4.10; N, 13.42. Found: C, 55.46; H, 4.24; N, 13.02.

The following compounds (**19b**, **20a** and **20b**) were prepared from **18** and the corresponding amines by a method similar to that described for **19a**.

5.13. 4-((3-Chloro-4-(3-(trifluoromethyl)phenoxy)phenyl)amino)-*N*-(2-(methylsulfonyl)ethyl)-8,9-dihydro-7H-pyrimido[4,5-*b*]azepine-6-carboxamide (**19b**)

Yield 40%, white crystals, mp 240–242 °C. ¹H NMR (DMSO-*d*₆) δ 2.64–2.75 (2H, m), 3.03 (3H, s), 3.27–3.41 (4H, m), 3.53–3.65 (2H, m), 7.14–7.24 (3H, m), 7.27 (1H, d, *J* = 9.1 Hz), 7.46 (1H, d, *J* = 8.0 Hz), 7.55–7.66 (2H, m), 7.73 (1H, t, *J* = 4.7 Hz), 7.92 (1H, d, *J* = 2.8 Hz), 7.99 (1H, s), 8.24 (1H, t, *J* = 5.5 Hz), 9.13 (1H, s). Anal. Calcd for C₂₅H₂₃ClF₃N₅O₄S: C, 51.59; H, 3.98; N, 12.03. Found: C, 51.60; H, 4.11; N, 11.87.

5.14. 4-((4-(1-Benzothiophen-4-yloxy)-3-chlorophenyl)amino)-N-(2-hydroxyethyl)-8,9-dihydro-7H-pyrimido[4,5-b]azepine-6-carboxamide (20a)

Yield 66%, white crystals, mp 220–222 °C. ^1H NMR (DMSO- d_6) δ 2.63–2.73 (2H, m), 3.24 (2H, q, J = 6.0 Hz), 3.29–3.39 (2H, m), 3.47 (2H, q, J = 6.0 Hz), 4.70 (1H, t, J = 6.0 Hz), 6.61 (1H, dd, J = 8.0, 0.7 Hz), 7.15 (1H, d, J = 8.9 Hz), 7.18 (1H, s), 7.31 (1H, t, J = 8.0 Hz), 7.48–7.57 (2H, m), 7.65 (1H, t, J = 4.6 Hz), 7.75 (1H, d, J = 8.0 Hz), 7.79 (1H, d, J = 5.7 Hz), 7.89 (1H, d, J = 2.5 Hz), 7.93–8.04 (2H, m), 9.07 (1H, s). Anal. Calcd for $\text{C}_{25}\text{H}_{22}\text{ClN}_5\text{O}_3\text{S}$ 0.5 H_2O : C, 58.08; H, 4.48; N, 13.55. Found: C, 58.26; H, 4.56; N, 13.44.

5.15. 4-((4-(1-Benzothiophen-4-yloxy)-3-chlorophenyl)amino)-N-(2-(methylsulfonyl)ethyl)-8,9-dihydro-7H-pyrimido[4,5-b]azepine-6-carboxamide (20b)

Yield 58%, white crystals, mp 254–255 °C. ^1H NMR (DMSO- d_6) δ 2.64–2.72 (2H, m), 3.03 (3H, s), 3.25–3.39 (4H, m), 3.59 (2H, q, J = 6.5 Hz), 6.61 (1H, dd, J = 8.0, 0.6 Hz), 7.15 (1H, d, J = 8.9 Hz), 7.21 (1H, s), 7.31 (1H, t, J = 8.0 Hz), 7.48–7.59 (2H, m), 7.70 (1H, t, J = 4.6 Hz), 7.75 (1H, d, J = 8.0 Hz), 7.79 (1H, d, J = 5.5 Hz), 7.90 (1H, d, J = 2.5 Hz), 7.98 (1H, s), 8.24 (1H, t, J = 5.4 Hz), 9.08 (1H, s). Anal. Calcd for $\text{C}_{26}\text{H}_{24}\text{ClN}_5\text{O}_4\text{S}_2$: C, 54.78; H, 4.24; N, 12.28. Found: C, 54.54; H, 4.30; N, 12.12.

5.16. HER2 and EGFR kinase assay

The cytoplasmic domain (amino acids 676–1255) of human HER2 and the cytoplasmic domain (amino acids 669–1210) of human EGFR were expressed as N-terminal peptide (DYKDDDD)-tagged protein using baculovirus expression system. The expressed HER2 kinase and EGFR kinase were purified by using anti-FLAG M2 affinity gel (Sigma–Aldrich, USA).

The HER2 and EGFR kinase assays were performed using radio labeled [γ - ^{32}P] ATP (GE Healthcare, USA) in 96 well plates. The kinase reactions were performed in 50 mmol/L Tris–HCl, pH 7.5, 5 mmol/L MnCl_2 , 0.01% Tween-20 and 2 mmol/L DTT containing 0.9 μCi of [γ - ^{32}P] ATP per reaction, 50 $\mu\text{mol/L}$ ATP, 5 $\mu\text{g/mL}$ poly-Glu-Tyr (4:1) and 0.25 $\mu\text{g/mL}$ of the purified HER2 or EGFR cytoplasmic domain in a total volume of 50 μL . To measure the IC_{50} value for enzyme inhibition, the compounds were incubated with the enzyme for 5 min prior to the reaction at room temperature. The kinase reactions were initiated by adding ATP. After the kinase reaction for 10 min at room temperature, the reactions were terminated by the addition of 10% (final concentration) trichloroacetic acid. The [γ - ^{32}P]-phosphorylated proteins were filtrated in Harvest plate (Millipore, USA) with a Cell harvester (PerkinElmer, USA) and washed free of [γ - ^{32}P] ATP with 3% phosphoric acid. The plates were dried, followed by the addition of 25 μL of Micro-Scint0 (PerkinElmer, USA). The radioactivity was counted by a Topcount scintillation counter (PerkinElmer, USA). IC_{50} values were calculated by nonlinear regression analysis.

5.17. Cell lines and culture

BT-474 cell line (HER2 over-expressing human breast cancer) was obtained from American Type Culture Collection. The BT-474 cells were cultured in RPMI 1640, and media supplemented with 10% heat-inactivated fetal bovine serum (FBS).

5.18. Cell growth assay

HER2 over-expressing human cancer cells (BT-474) were used for the cell growth assays. BT-474 cells were seeded into 48-mul-tiwell plates (3×10^4 cells/well) and allowed to attach overnight.

The cells were treated continuously with compounds for 5 days and then the live cell numbers were counted with a particle analyzer (CDA-500; Sysmex Corporation).

5.19. Kinase selectivity assay

The HER4 kinase assay was performed in the same method as the HER2 and EGFR kinase assays described above using 0.125 $\mu\text{g/mL}$ of HER4 cytoplasmic domain purchased from Upstate (USA).

Assays for the other 17 tyrosine kinases were performed using the Alphascreen[®] system (Perkin Elmer, USA) in 384-well plates. The cytoplasmic domains of VEGFR2 were expressed as N-terminal FLAG-tagged proteins using a baculovirus expression system. The full-length proteins of FAK and BMX were expressed as N-terminal FLAG-tagged proteins using a baculovirus expression system. FGFR3, VEGFR1 (Flt1), PDGFR α , PDGFR β , TIE2, c-Met, c-kit, Src, Lck, ZAP70, and InsR were purchased from Upstate (USA). FGFR1 was purchased from ProQinase (Germany). IGF-1R and CSK were purchased from BIOMOL (USA). Lyn A and Lyn B were purchased from Invitrogen (USA). The reaction conditions were optimized for each kinase: VEGFR2 (19 ng/mL of enzyme, 10 $\mu\text{mol/L}$ ATP, 10 min reaction, PY-100 conjugated acceptor beads [PY-100]); VEGFR1 (20 ng/mL of enzyme, 0.5 $\mu\text{mol/L}$ ATP, 5 min reaction, PT66 conjugated acceptor beads [PT-66]); FGFR1 (10 ng/mL of enzyme, 0.2 $\mu\text{mol/L}$ ATP, 10 min reaction, PY-100); FGFR3 (20 ng/mL of enzyme, 20 $\mu\text{mol/L}$ ATP, 10 min reaction, PY-100); PDGFR α (50 ng/mL of enzyme, 10 $\mu\text{mol/L}$ ATP, 30 min reaction, PT66); PDGFR β (50 ng/mL of enzyme, 20 $\mu\text{mol/L}$ ATP, 60 min reaction, PT66); InsR (100 ng/mL of enzyme, 10 $\mu\text{mol/L}$ ATP, 60 min reaction, PT66); TIE2 (20 ng/mL of enzyme, 2 $\mu\text{mol/L}$ ATP, 10 min reaction, PT66); c-Met (1 ng/mL of enzyme, 2 $\mu\text{mol/L}$ ATP, 10 min reaction, PT66); c-kit (10 ng/mL of enzyme, 20 $\mu\text{mol/L}$ ATP, 20 min reaction, PT66); IGF-1R (10 ng/mL of enzyme, 10 $\mu\text{mol/L}$ ATP, 20 min reaction, PT66); Src (0.33 ng/mL of enzyme, 2 $\mu\text{mol/L}$ ATP, 10 min reaction, PY-100); Lck (100 ng/mL of enzyme, 2 $\mu\text{mol/L}$ ATP, 30 min reaction, PY-100); BMX (6.6 ng/mL of enzyme, 2 $\mu\text{mol/L}$ ATP, 10 min reaction, PY-100); ZAP70 (30 ng/mL of enzyme, 2 $\mu\text{mol/L}$ ATP, 10 min reaction, PY-100); CSK (3.2 ng/mL of enzyme, 2 $\mu\text{mol/L}$ ATP, 10 min reaction, PY-100); FAK (62 ng/mL of enzyme, 2 $\mu\text{mol/L}$ ATP, 60 min reaction, PT66); Lyn A (2 ng/mL of enzyme, 2 $\mu\text{mol/L}$ ATP, 10 min reaction, PY-100); Lyn B (2.7 ng/mL of enzyme, 2 $\mu\text{mol/L}$ ATP, 10 min reaction, PY-100). The tyrosine kinase reactions were performed in 50 mmol/L Tris–HCl, pH 7.5, 5 mmol/L MnCl_2 , 5 mmol/L MgCl_2 , 0.01% Tween-20 and 2 mmol/L DTT, 0.1 $\mu\text{g/mL}$ biotinylated poly-Glu-Tyr (4:1) containing optimized concentration of enzyme, ATP as described above in a total volume of 25 μL . To determine IC_{50} values, the remaining kinase activities at seven concentrations (0.01, 0.1, 1, 10, 100, 1000, and 10,000 nmol/L) of compound were measured. Prior to the kinase reaction, test compound and enzyme were incubated for 5 min at room temperature. The reactions were initiated by adding ATP. After the reaction period as described above at room temperature, reactions were stopped by the addition of 25 μL of 100 mmol/L EDTA, 10 $\mu\text{g/mL}$ Alphascreen streptavidine donor beads and 10 $\mu\text{g/mL}$ acceptor beads described above in 62.5 mM HEPES, pH 7.4, 250 mmol/L NaCl, and 0.1% BSA. The plates were incubated in the dark for more than 12 h and read by an EnVision 2102 Multilabel Reader (PerkinElmer, USA) or a Fusion α Plate Reader (Packard, USA). Wells containing the substrate and the enzyme without the compound were used as total reaction control. Wells containing the biotinylated poly-Glu-Tyr (4:1) and the enzyme without ATP were used as basal control.

Assays for 16 serine/threonine kinases were performed using radiolabeled [γ - ^{33}P] ATP (GE Healthcare, USA) in 96-well plates. p38 α , ERK1, TAK1, ASK1, PKC θ , JNK1, MEK5, GSK3 β , B-raf, PLK1, and TTK were expressed as N-terminal FLAG tagged protein using a baculovirus expression system. IKK β and MEK1 were expressed as C-terminal FLAG tagged protein using a baculovirus expression

system. Aurora-B was expressed as N-terminal 6xHis tagged protein using a baculovirus expression system. MEK1 was expressed as N-terminal GST fusion protein using freestyle293 (Invitrogen, USA) expression. PKA was expressed using E.coli expression. The reaction conditions were optimized for each kinase: p38 α (100 ng/well of enzyme, 1 μ g/well of MBP (Wako, Japan), 0.1 μ Ci/well of [γ -³³P] ATP, 60 min reaction at 30 °C); ERK1 (100 ng/well of enzyme, 2 μ g/well of MBP, 0.1 μ Ci/well of [γ -³³P] ATP, 60 min reaction at 30 °C); MEK1 (25 ng/well of enzyme, 1 μ g/well of MBP, 0.1 μ Ci/well of [γ -³³P] ATP, 60 min reaction at 30 °C); TAK1 (30 ng/well of enzyme, 1 μ g/well of MBP, 0.1 μ Ci/well of [γ -³³P] ATP, 60 min reaction at 30 °C); ASK1 (30 ng/well of enzyme, 1 μ g/well of MBP, 0.1 μ Ci/well of [γ -³³P] ATP, 60 min reaction at 30 °C); PKC θ (25 ng/well of enzyme, 2 μ g/well of MBP, 0.1 μ Ci/well of [γ -³³P] ATP, 60 min reaction at 30 °C); JNK1 (10 ng/well of enzyme, 1 μ g/well of c-Jun, 0.1 μ Ci/well of [γ -³³P] ATP, 60 min reaction at 30 °C); MEK5 (3 ng/well of enzyme, 1 μ g/well of GST-ERK5 (K83 M), 0.3 μ Ci/well of [γ -³³P] ATP, 30 min reaction at 30 °C); GSK3 β (100 ng/well of enzyme, 0.2 μ g/well of pGS peptide, 0.1 μ Ci/well of [γ -³³P] ATP, 30 min reaction at room temperature); IKK β (20 ng/well of enzyme, 1 μ g/well of I κ B α , 0.1 μ Ci/well of [γ -³³P] ATP, reaction at room temperature); B-raf (25 ng/well of enzyme, 1 μ g/well of GST-MEK1 (K96R), 0.1 μ Ci/well of [γ -³³P] ATP, 20 min reaction at room temperature); MEK1 (100 ng/well of enzyme, 0.3 μ g/well of GST-ERK1 (K71A), 0.2 μ Ci/well of [γ -³³P] ATP, 20 min reaction at room temperature); Aurora-B (50 ng/well of enzyme, 30 μ mol/L of Aurora substrate peptide, 0.2 μ Ci/well of [γ -³³P] ATP, 60 min reaction at room temperature); PLK1 (80 ng/well of enzyme, 3 μ g/well of α -casein (usb, USA), 0.2 μ Ci/well of [γ -³³P] ATP, 40 min reaction at room temperature); TTK (120 ng/well of enzyme, 0.3 μ g/well of GST-MOBK1B, 0.2 μ Ci/well of [γ -³³P] ATP, 10 min reaction at room temperature); PKA (3 nmol/L of enzyme, 1 μ mol/L of PKA substrate peptide (Upstate, USA), 0.2 μ Ci/well of [γ -³³P] ATP, 10 min reaction at room temperature). Except for the PKC θ reaction, the serine/threonine kinase reactions were performed in 25 mmol/L HEPES, pH 7.5, 10 mmol/L magnesium acetate, 1 mmol/L DTT and 0.5 μ mol/L ATP containing optimized concentration of enzyme, substrate and radiolabeled ATP as described above in a total volume of 50 μ L. For the PKC θ reaction, enzyme reactions were performed in 25 mmol/L HEPES, pH 7.5, 10 mmol/L magnesium acetate, 1 mmol/L DTT, lipid activator (Upstate, USA) and 0.5 μ mol/L ATP containing optimized concentration of enzyme, substrate and radiolabeled ATP as described above in a total volume of 50 μ L. To determine IC₅₀ values, the remaining kinase activities at 5 concentrations (1, 10, 100, 1000, and 10,000 nmol/L) of compound were measured. Prior to the kinase reaction, compound and enzyme were incubated for 5 min at reaction temperature. The kinase reactions were initiated by adding ATP. After the reaction period as described above, the reactions were terminated by the addition of 10% (final concentration) trichloroacetic acid. The [γ -³³P]-phosphorylated proteins were filtrated in Harvest Plate (Millipore, USA) with a Cell Harvester (PerkinElmer, USA) and then free of [γ -³³P] ATP was washed out with 3% phosphoric acid. The plates were dried, followed by the addition of 40 μ L of MicroScintO (PerkinElmer, USA). Radioactivity was counted by a TopCount scintillation counter (PerkinElmer, USA). Wells containing the substrate and the enzyme without the compound were used as total reaction control. Wells containing the substrate and radiolabeled ATP without the enzyme were used as basal control. IC₅₀ values were calculated by nonlinear regression analysis.

5.20. 100-Fold dilution assay for HER2

A 1000 ng/ml (about 15 nmol/L) aliquot of HER2 kinase (Invitrogen, USA) and 10 \times IC₅₀ concentration of the inhibitor were

incubated together in kinase reaction buffer (50 mmol/L Tris-HCl, pH 7.5, 5 mmol/L MnCl₂, 0.01% Tween-20 and 2 mmol/L DTT) for 15 min at room temperature. This complex was diluted 1:100 into kinase reaction buffer containing 1 mmol/L ATP and 0.1 μ g/ml biotinylated poly-Glu-Tyr (4:1), and the kinase reaction began. After rapid dilution, concentrations of the enzyme and inhibitor were 10 ng/ml and 0.1 \times IC₅₀, respectively. The reaction was allowed to proceed for the indicated time and terminated by adding 500 mmol/L EDTA. After reaction, detection buffer (10 μ g/ml Alphascreen streptavidine donor beads and 10 μ g/ml acceptor beads conjugated with PY-100 in 62.5 mmol/L Hepes pH 7.4, 250 mmol/L NaCl, and 0.1% BSA) was added. The reaction plate was incubated in the dark for 16 h and then read by an EnVision plate reader (PerkinElmer, USA). The control reaction was performed without the inhibitor, which was replaced by an equal volume of DMSO.

5.21. 100-Fold dilution assay for EGFR

A 500 ng/ml (about 6 nmol/L) aliquot of EGFR kinase (Millipore, UK) and 10 \times IC₅₀ concentration of the inhibitor were incubated together in kinase reaction buffer (50 mmol/L Tris-HCl, pH 7.5, 5 mmol/L MnCl₂, 0.01% Tween-20 and 2 mmol/L DTT) for 60 min at room temperature. This complex was diluted 1:100 into kinase reaction buffer containing 1 mmol/L ATP and 0.1 μ g/ml biotinylated poly-Glu-Tyr (4:1), and the kinase reaction began. After rapid dilution, concentrations of the enzyme and inhibitor were 5 ng/ml and 0.1 \times IC₅₀, respectively. The reaction was allowed to proceed for the indicated time and terminated by adding 500 mmol/L EDTA. After reaction, detection buffer (10 μ g/ml Alphascreen streptavidine donor beads and 10 μ g/ml acceptor beads conjugated with PY-100 in 62.5 mmol/L Hepes pH 7.4, 250 mmol/L NaCl, and 0.1% BSA) was added. The reaction plate was incubated in the dark for 16 h and then read by an EnVision plate reader (PerkinElmer, USA). The control reaction was performed without the inhibitor, which was replaced by an equal volume of DMSO.

5.22. Determination of the configuration of 17

A colorless block (0.45 \times 0.41 \times 0.26 mm) was obtained by crystallization from 6 N HCl/methanol solution. A diffractometer Rigaku RAXIS RAPID was used with graphite monochromated Cu-K α radiation to obtain the following crystal data: C₉H₉ClN₃O₂⁺·Cl⁻·H₂O, crystal system triclinic, space group *P*-1 (#2), lattice parameters *a* = 6.359 Å, *b* = 9.141 Å, *c* = 10.545 Å, α = 100.41°, β = 96.99°, γ = 95.09°, *V* = 594.6 Å³, *Z* = 2, *T* = 298 K. Of the 6429 reflections collected, 2128 were unique (*R*_{int} = 0.054). The refinement converged with *R*₁ = 0.0625 and *wR*₂ = 0.1861 for 2003 reflections with *I* > 2 σ (*I*). The crystal contained one molecule of **17** and one molecule of water in the asymmetric unit. Further details of the X-ray structure data are available on request from the Cambridge Crystallographic Data Centre (deposition number CCDC 912741) (see Table 3).

5.23. Crystallization and structure determination

The human EGFR kinase domain was prepared as described previously.⁴ The complexes of EGFR with compounds were prepared by incubation of 5–10 mg/ml protein in the final buffer with a three fold molar excess of compound (in 100% DMSO) on ice for 2–3 h. Crystals suitable for data collection were obtained at 20 °C by sitting-drop vapor diffusion from a reservoir containing 20–25% PEG 3350, 0.2 M lithium sulfate, and 0.1 M MES (pH 5.5). Crystals were immersed in the reservoir solution containing 25% glycerol and flash-frozen with liquid nitrogen. Diffraction data were collected at the Advanced Light Source beamline 5.0.3. The

Table 3
X-ray data collection and refinement statistics

	Compound 20a	Compound 19b
<i>Data collection</i>		
Space group	$P2_12_12_1$	$P2_12_12_1$
<i>Unit cell dimensions</i>		
<i>a</i> , <i>b</i> , <i>c</i> (Å)	46.4, 68.3, 103.3	46.9, 69.2, 104.4
α , β , γ (°)	90, 90, 90	90, 90, 90
Resolution (Å)	50–1.80 (1.83–1.80)	50–1.70 (1.73–1.70)
Observed reflections	148,774	166,963
Unique reflections	30,817	38,002
Redundancy	4.8 (4.9)	4.4 (4.0)
Completeness (%)	99.7 (99.9)	99.7 (99.9)
I/σ (<i>I</i>)	26.1 (2.0)	26.2 (1.8)
R_{sym}^a	0.054 (0.898)	0.049 (0.810)
<i>Refinement</i>		
Resolution (Å)	40–1.80 (1.85–1.80)	40–1.70 (1.75–1.70)
Reflections	29,094	35,911
R_{cryst}^b	0.205 (0.282)	0.202 (0.327)
R_{free}^b	0.233 (0.292)	0.232 (0.381)
<i>Number of atoms</i>		
Proteins	2541	2450
Ligand/ion	44	40
Water	79	114
Average <i>B</i> value (Å ²)	32.7	26.2
<i>RMS deviation from ideal geometry</i>		
Bond lengths (Å)	0.009	0.009
Bond angles (°)	1.220	1.262
<i>Ramachandran plot (%)</i>		
Preferred regions	97.2	97.5
Allowed regions	1.4	2.2
Outliers	1.4	0.3
PDB code	3W32	3W33

^a $R_{\text{sym}} = \sum h \sum j | \langle I(h) \rangle - I(h) | / \sum h \sum j \langle I(h) \rangle$, where $\langle I(h) \rangle$ is the mean intensity of symmetry-related reflections.

^b $R_{\text{cryst}} = \sum | |F_{\text{obs}}| - |F_{\text{calc}}| | / \sum |F_{\text{obs}}|$. R_{free} was calculated for randomly chosen 5% of reflections excluded from refinement. Values in parentheses are for the highest resolution shell.

data were reduced and scaled using the HKL2000 software package.⁹ The structures were solved by molecular replacement with the program MOLREP¹⁰ of the CCP4 program suite¹¹ using the EGFR/TAK-285 structure (PDB code: 3POZ) as a search model. Several cycles of model building with Coot¹² and refinement with Refmac¹³ were performed for improving the quality of the model. The dictionary files for the ligands were prepared using AFITT (OpenEye Scientific Software, USA). The final models were validated using Molprobit.¹⁴ All structural figures were generated using PyMOL (Schrödinger, USA). Crystallographic processing and refinement statistics are summarized in Supplementary data. The coordinates and structure factors have been deposited in PDB with accession codes 3W33 and 3W32 for **19b** and **20a**, respectively (Table 3).

References and notes

- (a) Yamamoto, T.; Nishida, T.; Miyajima, N.; Kawai, S.; Ooi, T.; Toyoshima, K. *Cell* **1983**, *35*, 71; (b) Traxler, P. *Expert Opin. Ther. Targets* **2003**, *7*, 215; (c) Nagar, B.; Bornmann, W. G.; Pellicena, P.; Schindler, T.; Veach, D. R.; Miller, W. T.; Clarkson, B.; Kuriyan, J. *Cancer Res.* **2002**, *62*, 4236.
- (a) Petrov, K. G.; Zhang, Y. M.; Carter, M.; Cockerill, G. S.; Dickerson, S.; Gauthier, C. A.; Guo, Y.; Mook, R. A., Jr.; Rusnak, D. W.; Walker, A. L.; Wood, E. R.; Lackey, K. E. *Bioorg. Med. Chem. Lett.* **2006**, *16*, 4686; (b) Package Insert. *Tykerb (Lapatinib)*; GlaxoSmithKline: Research Triangle Park, NC 27709, USA, 2010; (c) Iqbal, S.; Goldman, B.; Fenoglio-Preiser, C. M.; Lenz, H. J.; Zhang, W.; Danenberg, K. D.; Shibata, S. I.; Blanke, C. D. *Ann. Oncol.* **2011**. <http://dx.doi.org/10.1093/annonc/mdl021>.

- (d) Whang, Y. E.; Armstrong, A. J.; Rathmell, W. K.; Godley, P. A.; Kim, W. Y.; Pruthi, R. S.; Wallen, E. M.; Crane, J. M.; Moore, D. T.; Grigson, G.; Morris, K.; Watkins, C. P.; George, D. J. *Urol. Oncol.* **2011**. <http://dx.doi.org/10.1016/j.urolonc.2010.09.018>. Epub ahead of print; (e) Mimura, K.; Kono, K.; Maruyama, T.; Watanabe, M.; Izawa, S.; Shiba, S.; Mizukami, Y.; Kawaguchi, Y.; Inoue, M.; Kono, T.; Choudhury, A.; Kiessling, R.; Fujii, H. *Int. J. Cancer* **2011**. <http://dx.doi.org/10.1002/ijc.25896>. Epub ahead of print; (f) Ross, H. J.; Blumenschein, G. R., Jr.; Aisner, J.; Damjanov, N.; Dowlati, A.; Garst, J.; Rigas, J. R.; Smylie, M.; Hassani, H.; Allen, K. E.; Leopold, L.; Zaks, T. Z.; Shepherd, F. A. *Clin. Cancer Res.* **2010**, *16*, 1938; (g) Ooi, A.; Takehana, T.; Li, X.; Suzuki, S.; Kunitomo, K.; Iino, H.; Fujii, H.; Takeda, Y.; Dobashi, Y. *Mod. Pathol.* **2004**, *17*, 895; (h) Tsou, H.-R.; Overbeek-Klumpers, E. G.; Hallett, W. A.; Reich, M. F.; Floyd, M. B.; Johnson, B. D.; Michalak, R. S.; Nilakantan, R.; Discifani, C.; Golas, J.; Rabindran, S. K.; Shen, R.; Shi, X.; Wang, Y.-F.; Upešlacis, J.; Wissner, A. *J. Med. Chem.* **2005**, *48*, 1107; (i) Li, D.; Shimamura, T.; Ji, H.; Chen, L.; Haringsma, H. J.; McNamara, K.; Liang, M.-C.; Perera, S. A.; Zaghlul, S.; Borgman, C. L.; Kubo, S.; Takahashi, M.; Sun, Y.; Chiriac, L. R.; Padera, R. F.; Lindeman, N. I.; Jänne, P. A.; Thomas, R. K.; Meyerson, M. L.; Eck, M. J.; Engelman, J. A.; Shapiro, G. I.; Wong, K.-K. *Cancer Cell* **2007**, *12*, 81; (j) Eskens, F. A. L. M.; Mom, C. H.; Planting, A. S. T.; Gietema, J. A.; Amelsberg, A.; Huisman, H.; van Doorn, L.; Burger, H.; Stopfer, P.; Verweij, J.; de Vries, E. G. *Br. J. Cancer* **2008**, *98*, 80; (k) Yokoi, K.; Thaker, P. H.; Yazici, S.; Rebhun, R. R.; Nam, D.-H.; He, J.; Kim, S.-J.; Abbruzzese, J. L.; Hamilton, S. R.; Fidler, I. J. *Cancer Res.* **2005**, *65*, 3716; (l) Wong, T. W.; Lee, F. Y.; Yu, C.; Luo, F. R.; Oppenheimer, S.; Zhang, H.; Smykla, R. A.; Mastalerz, H.; Fink, B. E.; Hunt, J. T.; Gavai, A. V.; Vite, G. D. *Clin. Cancer Res.* **2006**, *12*, 6186; (m) Mastalerz, H.; Chang, M.; Chen, P.; Dextraze, P.; Fink, B. E.; Gavai, A.; Goyal, B.; Han, W.-C.; Johnson, W.; Langley, D.; Lee, F. Y.; Marathe, P.; Mathur, A.; Oppenheimer, S.; Ruediger, E.; Tarrant, J.; Tokarski, J. S.; Vite, G. D.; Vyas, D. M.; Wong, H.; Wong, T. W.; Zhang, H.; Zhang, G. *Bioorg. Med. Chem. Lett.* **2007**, *17*, 2036; (n) Mastalerz, H.; Chang, M.; Gavai, A.; Johnson, W.; Langley, D.; Lee, F. Y.; Marathe, P.; Mathur, A.; Oppenheimer, S.; Tarrant, J.; Tokarski, J. S.; Vite, G. D.; Vyas, D. M.; Wong, H.; Wong, T. W.; Zhang, H.; Zhang, G. *Bioorg. Med. Chem. Lett.* **2007**, *17*, 2828; (o) Mastalerz, H.; Chang, M.; Chen, P.; Fink, B. E.; Gavai, A.; Han, W. C.; Johnson, W.; Langley, D.; Lee, F. Y.; Leavitt, K.; Marathe, P.; Norris, D.; Oppenheimer, S.; Slecicka, B.; Tarrant, J.; Tokarski, J. S.; Vite, G. D.; Vyas, D. M.; Wong, H.; Wong, T. W.; Zhang, H.; Zhang, G. *Bioorg. Med. Chem. Lett.* **2007**, *17*, 4947; (p) Bhattacharya, S. K.; Cox, E. D.; Kath, J. C.; Mathiowetz, A. M.; Morris, J.; Moyer, J. D.; Pustilnik, L. R.; Rafidi, K.; Richter, D. T.; Su, C.; Wessel, M. D. *Biochem. Biophys. Res. Commun.* **2003**, *307*, 267; (q) Jani, J. P.; Finn, R. S.; Campbell, M.; Coleman, K. G.; Connell, R. D.; Currier, N.; Emerson, E. O.; Floyd, E.; Harriman, S.; Kath, J. C.; Morris, J.; Moyer, J. D.; Pustilnik, L. R.; Rafidi, K.; Ralston, S.; Rossi, A. M.; Steyn, S. J.; Wagner, L.; Winter, S. M.; Bhattacharya, S. K. *Cancer Res.* **2007**, *67*, 9887; (r) Ripin, D. H. B.; Bourassa, D. E.; Brandt, T.; Castaldi, M. J.; Frost, H. N.; Hawkins, J.; Johnson, P. J.; Massett, S. S.; Neumann, K.; Phillips, J.; Raggon, J. W.; Rose, P. R.; Rutherford, J. L.; Sitter, B.; Stewart, A. M., III; Vetelino, M. G.; Wei, L. *Org. Process Res. Dev.* **2005**, *9*, 440; (s) Lippa, B.; Kauffman, G. S.; Arcari, J.; Kwan, T.; Chen, J.; Hungerford, W.; Bhattacharya, S.; Zhao, X.; Williams, C.; Xiao, J.; Pustilnik, L.; Su, C.; Moyer, J. D.; Ma, L.; Campbell, M.; Steyn, S. *Bioorg. Med. Chem. Lett.* **2007**, *17*, 3081.
- (a) Ishikawa, T.; Seto, M.; Banno, H.; Kawakita, Y.; Oorui, M.; Taniguchi, T.; Ohta, Y.; Tamura, T.; Nakayama, A.; Miki, H.; Kamiguchi, H.; Tanaka, T.; Habuka, N.; Sogabe, S.; Aertgeerts, K.; Kamiyama, K. *J. Med. Chem.* **2011**, *54*, 8030; (b) Doi, T.; Takiuchi, H.; Ohtsu, A.; Fuse, N.; Goto, M.; Yoshida, M.; Dote, N.; Kuze, Y.; Jinno, F.; Fujimoto, M.; Takubo, T.; Nakayama, N.; Tsutsumi, R. *Br. J. Can.* **2012**, *106*, 1.
- Aertgeerts, K.; Skene, R.; Yano, J.; Sang, B.; Zou, H.; Snell, G.; Jennings, A.; Iwamoto, K.; Habuka, N.; Hirokawa, A.; Ishikawa, T.; Tanaka, T.; Miki, H.; Ohta, Y.; Sogabe, S. *J. Biol. Chem.* **2011**, *21*, 18756.
- (a) Ikemoto, T.; Ito, T.; Nishiguchi, A.; Tomimatsu, K. *Tetrahedron* **2004**, *60*, 10851–10857; (b) Ikemoto, T.; Ito, T.; Nishiguchi, A.; Tomimatsu, K. *Tetrahedron Lett.* **2004**, *45*, 9335–9339; (c) Seto, M.; Miyamoto, N.; Aikawa, K.; Aramaki, Y.; Kanzaki, N.; Izawa, Y.; Baba, M.; Shiraiishi, M. *Bioorg. Med. Chem.* **2005**, *13*, 363–386.
- Clark, J.; Parvizi, B.; Southon, W. I. *J. Chem. Soc., Perkin Trans. 1* **1976**, *2*, 125.
- Kawakita, Y.; Banno, H.; Ohashi, T.; Tamura, T.; Yusa, T.; Nakayama, A.; Miki, H.; Iwata, H.; Kamiguchi, H.; Tanaka, T.; Habuka, N.; Sogabe, S.; Ohta, Y.; Ishikawa, T. *J. Med. Chem.* **2012**, *55*, 3975.
- Iwata, H.; Imamura, S.; Hori, A.; Hixon, M. S.; Kimura, H.; Miki, H. *Biochemistry* **2011**, *50*, 738.
- Otwinski, Z.; Minor, W. *Methods Enzymol.* **1997**, *276*, 307.
- Vagin, A.; Teplyakov, A. *J. Appl. Crystallogr.* **1997**, *30*, 1022.
- Bailey, S. *Acta Crystallogr.* **1994**, *D50*, 760.
- Emsley, P.; Lohkamp, B.; Scott, W. G.; Cowtan, K. *Acta Crystallogr.* **2010**, *D66*, 486.
- Murshudov, G. N.; Vagin, A. A.; Dodson, E. J. *Acta Crystallogr.* **1997**, *D53*, 240.
- Chen, V. B.; Arendall, W. B., 3rd; Headd, J. J.; Keedy, D. A.; Immormino, R. M.; Kapral, G. J.; Murray, L. W.; Richardson, J. S.; Richardson, D. C. *Acta Crystallogr.* **2010**, *D66*, 12.